Aerosol and Air Quality Research, 13: 1181–1196, 2013

ISSN: 1680-8584 print / 2071-1409 online
doi: 10.4209/aaqr.2013.02.0060

Long Term Black Carbon Measurements at Two Urban Locations in New York

Oliver V. Rattigan[1*], Kevin Civerolo[1], Prakash Doraiswamy[2+], H. Dirk Felton[1], Philip K. Hopke[3]

[1] *New York State Department of Environmental Conservation, Division of Air Resources, 625 Broadway, Albany, NY, USA*
[2] *Atmospheric Sciences Research Center, University at Albany, Albany, NY, USA*
[3] *Center for Air Resources Engineering and Science, Clarkson University, Potsdam, NY, USA*

ABSTRACT

Measurements of $PM_{2.5}$ black carbon (BC) over an 8–9 year period are used to characterize temporal patterns at sites in New York City (NYC) and Rochester, NY. Annual mean BC at the NYC location ranges from 1.4 to 2.0 μg/m^3, whereas mean concentrations at Rochester are approximately a factor of 2–3 lower. BC amounts to 15–20% of $PM_{2.5}$ mass in NYC compared to 7–10% at Rochester. Seasonal patterns reveal the highest BC concentrations in NYC from November to February versus June to November at Rochester. At both locations, mean weekday (Monday-Friday) BC concentrations are statistically higher compared to weekends (Saturday and Sunday). Weekday BC diurnal profiles exhibit a morning peak between 6–10 AM EST followed by an afternoon minimum, with a secondary peak in the late evening. Sunday BC diurnal profiles show highest concentrations at night, from 8 PM to 2 AM. These patterns are consistent with vehicle counts on nearby roadways and boundary layer dynamics at both locations. Simultaneous measurements of BC at 370 and 880 nm show an enhancement in BC_{370} relative to the BC_{880} from October to March. This enhanced signal is most evident at Rochester during late evening and early morning hours (8 PM to 4 AM) on weekends, and is attributed to UV absorbing species (such as wood smoke markers) in the ambient particle mixture. At the NYC site, the levels of Nickel (Ni) and Cobalt (Co) in PM_{10} are elevated during the heating season due to residual oil combustion. The long term datasets are used to explore the seasonal relationship between BC_{880} and EC at both sites.

***Keywords*:** Black carbon; Aethalometer®; Diurnal pattern; Wood smoke; Nickel.

INTRODUCTION

Black carbon (BC) generally refers to the portion of ambient particles that absorbs strongly in the visible and near infrared. This quantity is also referred to as "light absorbing carbon" or LAC (Malm *et al.*, 1994). Elemental carbon (EC) is operationally defined by thermal optical analysis methods whereby a particulate sample is oxidized and the evolved gas quantified relative to a fixed methane concentration (Birch and Cary, 1996; Chow *et al.*, 2007). Since BC and EC are method dependent definitions simultaneous measurements are not necessarily equivalent due to variations in optical properties of the ambient aerosol depending on the composition, source, and degree of aging (Liousse *et al.*, 1993; Jeong *et al.*, 2004; Park *et al.*, 2006; Salako *et al.*, 2012). Interferences from organic species (Wallen *et al.*, 2010) can impact thermo-optical measurements of EC. BC or EC are produced from fossil fuel combustion in, for example, motor vehicles including diesel engines, heating and biomass burning (Hildemann *et al.*, 1991; Seinfeld and Pandis, 1998 and references therein; Schauer, 2003; Bond *et al.*, 2007) and are considered indicators of primary combustion emissions. In the US, approximately 50% of BC emissions are from the transportation sector with the majority from diesel combustion sources (http://www.epa.gov/blackcarbon).

Carbonaceous particles can play an important role in climate processes (Jacobson 2002; IPCC 2007; Ramanthan and Carmichael 2008) alter cloud properties (Albrecht, 1989), impact air quality and human health. Residents living near major roadways and exposed to vehicle combustion particles including BC may be at increased risk for respiratory symptoms and reduced lung function (Kim *et al.*, 2004; Cornell *et al.*, 2012). Measurements of BC are important in order to understand the major sources and subsequent evolution in the atmosphere. Long term measurements are of key interest in the evaluation of emission control measures and to assess impacts on health and climate.

Several different optical methods are used to measure

* Corresponding author.
E-mail address: ovrattig@gw.dec.state.ny.us
+ Now at RTI International, Research Triangle Park, NC, USA

BC. Among the time-resolved filter based methods, the Aethalometer® (Hansen *et al.*, 1984) is one of the most extensively used instruments. Alternative filter based methods include the Multiangle Absorption Photometer, MAAP (Petzold *et al.*, 2002), and the Particle Soot Absorption Spectrometer, PSAP (Bond *et al.*, 1999). These methods operate by measuring a change in optical light transmission through a fiber filter as it samples ambient particles. The optical response of these instruments may depend on the mixing state of black carbon particles. For example optical saturation under heavy BC loadings leads to an underestimation in concentration and interference from particles other than BC may contribute to light absorption (Kirchstetter *et al.*, 2004). The data presented here have been corrected for optical saturation using the Virkkula *et al.* (2007) algorithm. In the US BC has been measured (using the Aethalometer®) along with certain hazardous air pollutants (HAPs) at key areas (predominantly urban) designated as National Air Toxics Trends Station (NATTS) sites (listed at http://www.epa.gov/ttn/amtic/natts.html). This monitoring program was designed to characterize trends in ambient HAP levels in support of human exposure assessments and for the evaluation of emission control strategies.

The focus of this paper is to characterize the temporal patterns in $PM_{2.5}$ BC using long-term measurements from two urban locations in New York. The data were used to examine annual, seasonal, day of week and diurnal patterns and the relationship with co-pollutants in an effort to understand major source impacts. In addition, we explore the seasonal relationship between BC and EC from different measurement methods.

METHODS

New York City, Bronx

The ambient air monitoring site in New York City is at Intermediate School 52 (IS 52), 681 Kelly Street in the South Bronx, NY (Rattigan *et al*, 2010). The site grid reference is 40°48'57"N and 73°54'07"W and the USEPA site identification code is 36-005-0110. This site lies in a mainly residential area but is impacted by traffic from several nearby highways. These include the Bruckner Expressway (I-278) approximately 0.5 km to the southeast and Interstates 87 (Major Deegan), 895 and 95 all which lie within 1–3 km of the site. The New York State Department of Transportation (http://www.dot.ny.gov) annual average daily traffic (AADT) counts on these roadways range from 110,000–160,000. Hunts Point produce market and Oak Point freight yard are within 1–2 km of the site, leading to significant heavy duty diesel truck traffic on connecting roadways. The Bronx has a total population of approximately 1.3 million inhabitants. The site is one of two NATTS sites in New York and contains an extensive set of ambient monitoring equipment for gaseous and particle sampling (http://www.dec.ny.gov/airmon). Air sampling at the site was suspended for an approximate two year period from July 2010 to June 2012 due to roof repair work. During this period measurements of BC were carried out at a site approximately 7 km to the northwest (site identification code 36-005-0080).

Rochester

Rochester lies on the southern shore of Lake Ontario approximately 400 km northwest of New York City. Ambient measurements are performed at the New York State Department of Environmental Conservation (NYS DEC) site in Rochester, New York (43°08'46"N, 77°32'52"W). Equipment is housed in or positioned on the rooftop of an air conditioned shelter located on National Grid property off Yarmouth Road (Wang *et al.*, 2010). This site is the second NATTS site in the state (USEPA site identification code 36-055-1007). The site is located in Brighton on the east side of the urban center adjacent to the intersection (~300 m) of two major highways (I-490 and I-590) with AADT counts ranging from 100,000–120,000. Recent estimates indicate the population of Rochester is approximately 210,500 (U.S. Census Bureau, http://www.census.gov/), making it the third largest city in New York State.

BC Instrumentation

Black carbon measurements began at the Bronx site in May 2003 and at the Rochester site in May 2004. At both sites a Magee Scientific, model AE-21, dual wavelength (880 nm and 370 nm) Aethalometer® (Hansen *et al.*, 1984) sampled $PM_{2.5}$ particles through a BGI model 1.828 sharp cut cyclone at 5 LPM onto a quartz fiber filter tape (Pallflex®). The Aethalometer® calculates light attenuation (ATN) due to particle deposit on the filter relative to a clean part of the filter. By measuring the rate of change in light attenuation assumed due solely to absorption by BC the mass concentration is determined. A 5 min time interval and an absorption coefficient of 16.6 m^2/g at 880 nm were used in this study. However, the relationship between ATN and BC may become non-linear (Petzold *et al.*, 1997; Bond *et al.*, 1999; Weingartner *et al.*, 2003; Arnott *et al.*, 2005; Turner *et al.*, 2007; Virkkula *et al.*, 2007; Park *et al.*, 2010). The Aethalometer® accumulates sample on a portion of the filter tape and as the BC loading increases a change in the optical properties of the particle laden filter causes the ATN to BC response to become non-linear. This manifests itself in a saw-tooth like signal, where the BC concentration increases immediately following a tape advance, i.e., ATN is lowest, and BC is progressively underestimated as the loading increases. The empirical algorithm developed by Virkkula *et al.* (2007) attempts to correct for this effect;

$$BC_{corrected} = (1 + K \times ATN)BC_0 \quad (1)$$

where K is the correction factor and BC_0 is the uncorrected BC. The correction factor was calculated for each filter spot i, using the average of the last two data points of spot i and the first two data points of spot i + 1 according to Eq. (2);

$$K_i = \frac{1}{ATN\left(t_{i,last}\right)} \times \left[\frac{BC_0\left(t_{i+1,first}\right)}{BC_0\left(t_{i,last}\right)} - 1\right] \quad (2)$$

Five minute Aethalometer® raw data were corrected and processed into hourly intervals using software developed by the Air Quality Laboratory at Washington University (Turner *et al.*, 2007).

A Thermo Scientific model 5012 MAAP was also used for measurements of BC (670 nm) over an approximately two and a half year period, 2007–2009, at the Bronx site. The MAAP sampled particles through a $PM_{2.5}$ sharp cut cyclone at 16.7 LPM onto a glass fiber filter tape (Whatman®, GF10). Visible light from a 670 nm source was directed onto the particle laden filter. Light transmitted through the filter into the forward hemisphere and reflected into the back hemisphere was measured by a series of photodetectors. A radiative transfer algorithm accounted for multiple scattering effects (Petzold *et al.*, 2002). A mass absorption cross section of 6.6 m^2/g at 670 nm was used to estimate the BC concentration.

Co-Pollutant Measurements

Bronx Site: A model 3 Sunset Laboratory Inc. OCEC carbon aerosol analyzer collected particles through a BGI, model SCC 2.354, $PM_{2.5}$ sharp cut cyclone at 8 LPM which provided hourly measurements of EC and OC (Rattigan *et al.*, 2010). Interagency for Monitoring Protected Visual Environments (IMPROVE) 24 h integrated $PM_{2.5}$ particle sample collection (Malm *et al.*, 1994) for chemical analysis was also carried out at the Bronx site from 2004 to 2010. IMPROVE carbon samples were analyzed according to the thermal optical reflectance (TOR) method (Chow *et al.*, 2007). Ambient measurements of nitrogen oxides, (NO, NO_2 and NO_x = NO + NO_2), SO_2 and O_3 were made using Thermo Scientific gas analyzers, models 42C, 43C and 49C, respectively. Hourly $PM_{2.5}$ total mass was measured using a Thermo Scientific Tapered Element Oscillating Microbalance (TEOM) model 1400ab. Sub-hourly measurements of $PM_{2.5}$ sulfate and nitrate were made using a Thermo Scientific model 5020i Sulfate Particulate Analyzer and a Rupprecht & Patashnick Co., Inc., model 8400N Ambient Particle Nitrate Monitor, respectively.

Measurements of SO_2, CO, O_3 and $PM_{2.5}$ mass are recorded on hourly intervals at Rochester. At both sites 24 h integrated carbonaceous measurements were made every third day employing the Chemical Speciation Network (CSN) sampling protocol allowing for a comparison between BC and EC. Two different CSN sampling and analysis protocols are used for 24 h carbon sampling as described previously (Rattigan *et al.*, 2011). CSN 24 h carbon sampling was carried out using either a Rupprecht and Patashnick Co. Inc. Partisol model 2300 Speciation Sampler (R&P 2300) or a Spiral Aerosol Speciation Sampler, Met One Instruments (MetOne). Both instruments employed prefired 47 mm diameter Whatman® QMA quartz fiber filters with analysis based on the NIOSH 5040 thermal optical transmission (TOT) protocol (Peterson and Richards, 2002). CSN 24 h carbon filter sampling was changed to the URG-3000N Sequential Particulate Speciation System, (URG) in May 2007 at the Bronx and in April 2009 at Rochester. The URG-3000N uses a similar protocol to the IMPROVE with 25 mm Pallflex® Tissuquartz filters and analysis based on the IMPROVE_A thermal optical reflectance (TOR) method (Chow *et al.*, 2007). Chemical speciation sampling at the Bronx ceased in June 2010. $PM_{2.5}$ mass was collected over 24 h periods using the Thermo Scientific Partisol Plus 2025 Sequential Ambient Particle Sampler. PM_{10} samples were also collected over 24 h periods using a Partisol Plus 2025 sampler every 6th day and analyzed for selected trace metals. Sample inlets were positioned 2 m above rooftop (approximately 15 m above ground level at the Bronx and 5 m at Rochester).

Planetary Boundary Layer Heights

The planetary boundary layer (PBL) heights were calculated in the Nonhydrostatic Mesoscale Model of the Weather Research and Forecasting System (WRF-NMM) using the Mellor-Yamada-Janjic Parameterization (Janjic, 2001). The weather forecast product consisted of the 12:00 coordinated universal time cycle forecasts of the National Center for Environmental Prediction (NCEP) operational 12-km, WRF-NMM based North American Mesoscale model, which had already been processed by the NCEP WRF postprocessor. PBL heights were extracted for the grid cells in which the air monitoring stations were located (Doraiswamy *et al.*, 2010).

RESULTS AND DISCUSSION

Aethalometer® Loading Correction Factor and Comparison to MAAP

BC_{880} data were corrected for particle loading based on the Virkkula *et al.* (2007) method. Mean K factors at 880 nm from Eq. (2) varied from approximately 0.001 in summer (June, July and August) to 0.012 in winter (December, January and February) at the Bronx (Fig. 1) and 0.0015 to 0.008 at Rochester. This amounted to a correction in BC_{880} ranging from approximately 50% in winter to 15% in summer. The seasonal variation in the K factor over a two year period at the Bronx is shown along with 24 h integrated sulfate and the OC/EC ratio in Fig. 1. A higher contribution of scattering components e.g., sulfate and secondary organic carbon to the total particle mass in summer offsets the loading effect as previously indicated (Weingartner *et al.*, 2003; Virkkula *et al.*, 2007). A negative K indicates the raw BC data are overestimated. Hourly Aethalometer® BC_{880} (raw and corrected) data are compared to MAAP BC at the Bronx in Fig. 2. Mean MAAP BC was 50% higher than raw Aethalometer® BC_{880} data from November to February and around 15% higher from June to September. Following correction of the Aethalometer® data the monthly differences were within the 2 σ confidence intervals as indicated in Fig. 2.

Annual Trends

Hourly BC_{880} corrected for particle loading are shown as box and whisker plots in Fig. 3; Bronx data in Fig. 3(a) and Rochester Fig. 3(b). A comparison of annual BC_{880} concentrations and other co-pollutants at the Bronx and Rochester are shown in Table 1 and Table 2, respectively. Annual mean BC_{880} at the Bronx was 2.0 $\mu g/m^3$ during

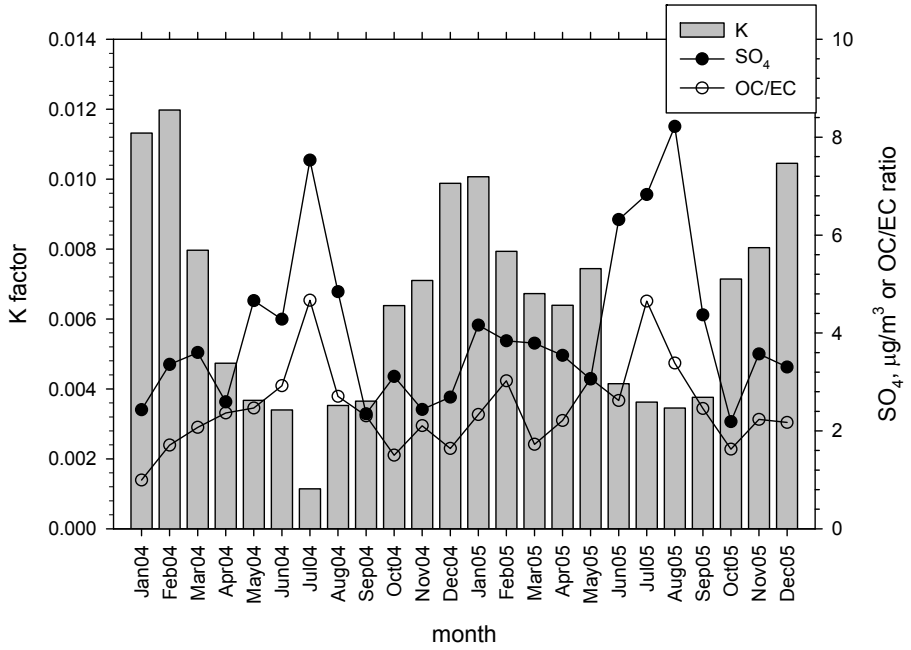

Fig. 1. Comparison of mean monthly K factors for 880 nm, 24-h integrated SO_4 and OC/EC ratio during 2004–2005 at the Bronx.

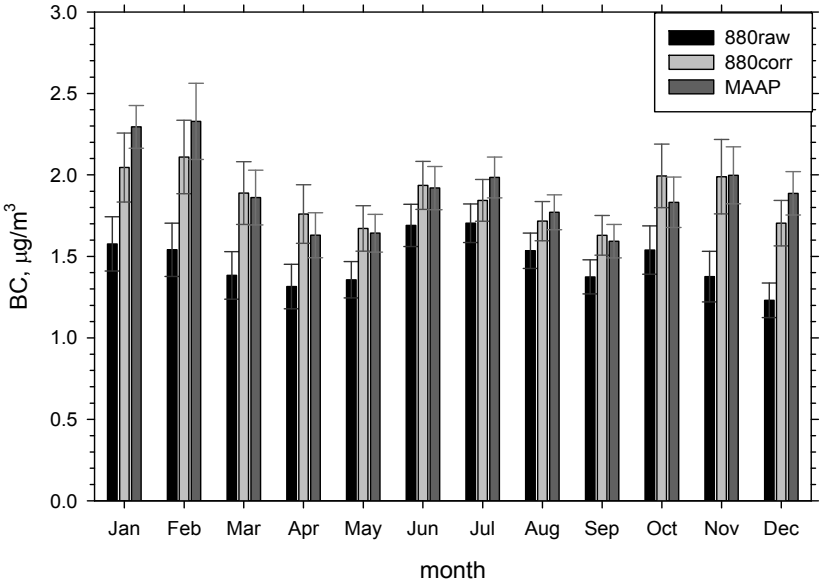

Fig. 2. Comparison of mean Aethalometer® BC_{880} raw (black), BC_{880} corrected (light grey) and the MAAP BC (dark grey) at the Bronx. The error bars denote the 95% confidence limits.

2003–2004 but concentrations were 15% lower in 2005 (significant at the 95% CI, $p < 0.05$). Concentrations remained relatively uniform within 3% between 2005 and 2008 with a slightly higher variation of 6% from 2008 to 2011. However, BC_{880} was 20% lower in 2012. Most other pollutants show a more uniform downward trend. For example, SO_2 and NO_x decreased by 4.6 and 8 ppb respectively, between 2005 and 2009 amounting to an approximate 40% reduction in both cases. $PM_{2.5}$ mass declined steadily throughout the period decreasing by 4 µg/m^3 (30%) since 2003. The majority of the $PM_{2.5}$ mass reduction is attributed to $PM_{2.5}$ sulfate which dropped by 2–3 µg/m^3 (if ammonium sulfate is considered) and nitrate which decreased by approximately 0.7 µg/m^3. These reductions are attributed to federal SO_2 and NO_x emission controls (National Emissions Inventory (NEI) summary obtained from http://www.epa.gov/ttn/chief/trends/index.html) during the past decade that had a large impact on emissions from coal burning power utilities resulting in a decrease in $PM_{2.5}$ particle species across the eastern US. BC_{880} at the Bronx amounted to approximately 14–20% of total $PM_{2.5}$ mass, Fig. S1(a).

Annual mean BC_{880} at Rochester, Fig. 3(b), was approximately a factor of 2–3 lower than the Bronx varying between 0.70 to 0.76 μg/m^3 during 2004 and 2007. Thereafter BC_{880} decreased reaching 0.57 μg/m^3 in 2009 with a further drop to 0.46 μg/m^3 in 2010 representing a 30% decrease in BC_{880} since 2007. Mean BC_{880} for 2011

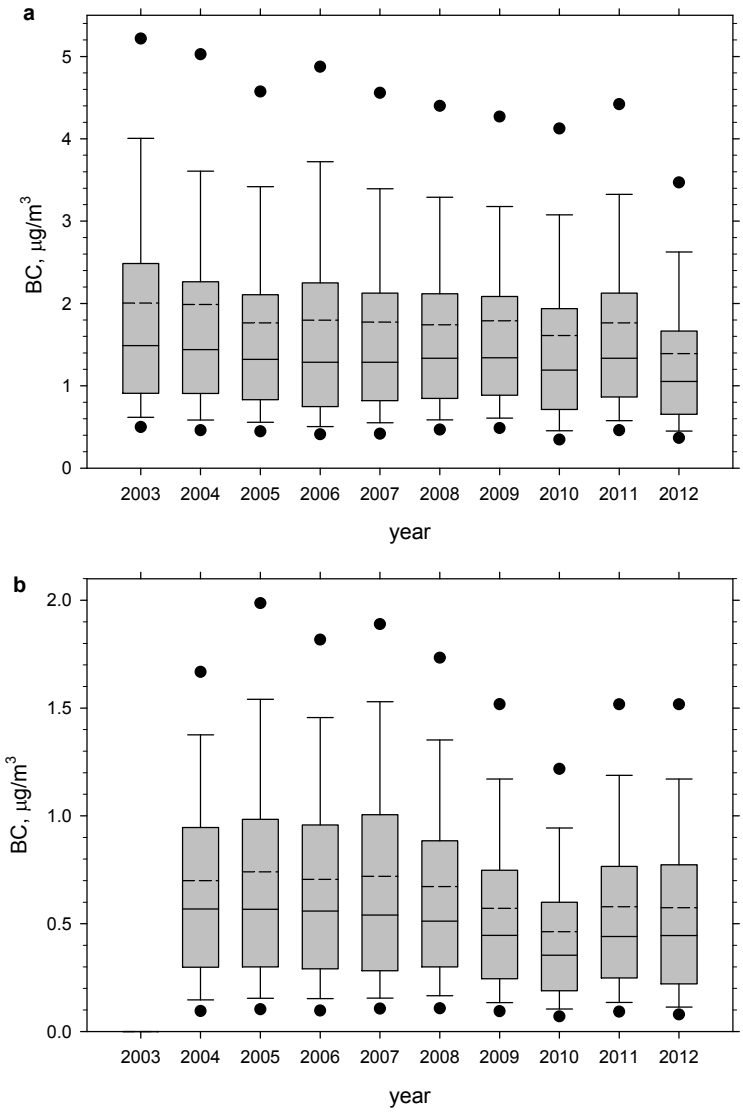

Fig. 3. Box and whisker plot of annual BC_{880} concentrations in μg/m^3 at (a) the Bronx and (b) Rochester. The boxes represent the 25th percentile (lower edge), median (solid line), mean (dashed line) and 75th percentile (upper edge). Whiskers represent the 10th and 90th percentiles and the solid circles represent the 5th and 95th percentiles.

Table 1. Annual mean concentration of selected pollutants at the Bronx.

Year	BC (μg/m^3)	SO_2 (ppb)	NO_x (ppb)	$PM_{2.5}$ (μg/m^3)	SO_4 (μg/m^3)	NO_3 (μg/m^3)
2003	2.04	8.6	49.6	14.8	4.37	2.37
2004	1.99	10.3	21.6	13.7	3.71	2.09
2005	1.72	10.9	21.0	13.8	4.49	2.20
2006	1.69	8.83	17.1	12.6	3.69	1.90
2007	1.67	7.86	16.0	12.7	4.07	2.15
2008	1.71	6.58	14.3	11.8	3.44	1.90
2009	1.81	6.33	13.1	10.8	2.57	1.67
2010	1.61	6.68	14.0	10.2	2.39	1.68
2011	1.76	a	a	a	a	a
2012	1.39	2.42	10.5	10.0	a	a

[a] No data.

Table 2. Annual mean concentrations of selected pollutants at Rochester.

Year	BC (μg/m^3)	EC (μg/m^3)	SO_2 (ppb)	CO (ppb)	$PM_{2.5}$ (μg/m^3)	SO_4 (μg/m^3)	NO_3 (μg/m^3)
2004	0.70	0.39	4.58	468.8	11.0	3.27	1.82
2005	0.76	0.45	4.20	461.6	12.5	3.65	1.91
2006	0.71	0.42	4.18	495.6	9.5	2.87	1.43
2007	0.72	0.51	4.07	426.0	9.9	3.29	1.50
2008	0.67	0.48	2.91	388.0	9.0	2.64	1.58
2009	0.57	0.46	2.54	420.4	7.6	1.92	1.42
2010	0.46	0.44	2.19	428.8	8.4	1.77	1.04
2011	0.58	0.47	1.22	189.6	9.2	1.76	1.13
2012	0.57	0.66	1.04	208.0	8.7	1.60	1.05

and 2012 however were similar to 2009. SO_2 at Rochester varied little between 2004 and 2007 (4.6–4.1 ppb) but concentrations declined steadily thereafter reaching 1.0 ppb in 2012, amounting to a total decrease of 75%. The shutdown of the Russell Station coal-fired power plant in 2008 contributed to decreases in various pollutant concentrations in the region (Wang *et al.*, 2011a). Similar to the Bronx $PM_{2.5}$ total mass dropped by approximately 3 μg/m^3 between 2005 and 2010 mostly attributed to a reduction in $PM_{2.5}$ SO_4. These improvements in air quality are due to a combination of point source and diesel fuel emission controls (Wang *et al.*, 2010, 2011a, 2012). The downturn in the economy may also have contributed to some of these changes. BC_{880} averaged 7–9% of $PM_{2.5}$ mass at Rochester on an annual basis, shown in Fig. S1(b). BC concentrations reported here are similar to other locations in the USA (Jeong *et al.*, 2004; Lough *et al.*, 2006; Park *et al.*, 2006) and Europe (Saha and Despiau, 2009) but lower than those observed at some Asian sites (Baxla *et al.*, 2009; Begum *et al.*, 2012; Salako *et al.*, 2012; Swamy *et al.*, 2012).

Monthly Pattern

Monthly data presented in Fig. 4(a) show that maximum BC_{880} at the Bronx occurs from November to February as represented by the 95 percentiles with a secondary maximum in June and July. The former is attributed to lower boundary layer heights and increased emissions from space heating use in colder periods and the latter to increased emissions from outdoor activity such as vehicles, construction work and outdoor food grilling. The fraction of BC_{880} to $PM_{2.5}$ mass is lowest in July (mean 12%) reflecting the higher contribution of secondary aerosol to $PM_{2.5}$ mass during summer compared to other periods, Fig S2(a). In contrast BC_{880} at Rochester is highest from June to November, with maximum concentrations in November, Fig. 4(b). This pattern reflects increased summer activity and increased emissions from space heating sources such as wood burning with the onset of colder periods in October and November (Wang *et al.*, 2011b). With the advancement of winter and snow cover over outdoor wood storage piles there is a preference for natural gas over wood burning for space heating. The proportion of BC_{880} to $PM_{2.5}$ mass is highest in autumn, Fig. S2(b), reflecting increased space heating use with the onset of colder periods. Maximum BC was also observed from November to February at urban locations in the USA (Park *et al.*, 2006), Europe (Saha and Despiau, 2009) India and Bangladesh (Baxla *et al.*, 2009; Begum *et al.*, 2012; Swamy *et al.*, 2012). However in Hong Kong maximum BC was found from July to September (Cheng *et al.*, 2012) indicating sources other than nearby traffic was impacting the site during the summer period. A larger seasonal gradient in BC was observed at the Asian locations, factor of 3 to 5 change, compared to 40 to 50% in New York.

Weekday/Weekend Pattern

BC_{880} day of week pattern versus season at the Bronx shows concentrations are highest on weekdays, Monday-Friday and lowest on Sundays with Saturdays in between, Fig. 5. The most pronounced Sunday/weekend difference is in spring and summer with differences of 40–45%, whereas the least difference is in winter (20%). Two sample t-tests show mean weekday BC_{880} concentrations are higher compared to those on a Saturday or Sunday, significant at the 95% CI ($p < 0.05$). In addition concentrations on Saturday are significantly higher than on Sunday. NO_x concentrations show a similar pattern to BC_{880} and are approximately 40% higher on a weekday versus a Sunday in spring, summer and 20% higher in winter, Fig. 6. Mean weekday SO_2 is approximately 20% higher than on Sundays in spring and summer but no discernable weekday to weekend difference are observed in autumn and winter. The different SO_2 day of week pattern reflects additional emissions from sources other than traffic such as fuel oil combustion (used for heating water and space heating) which has no particular day of week pattern. Mean daily vehicle counts on the nearby Bruckner Expressway during 2008 varied from 110,000 to 135,000 with Sundays the lowest, but not significant at the 95% confidence interval. Therefore, it is unlikely that the small differences in daily vehicle counts could explain the different weekday versus weekend BC_{880} pattern at the Bronx. BC_{880} at Rochester is also lower on Sunday compared to weekdays varying from 20% lower in winter to 37% during spring, Fig. S3. At Rochester however, there is a significant difference between weekday and weekend daily vehicle counts which could explain differences in BC_{880} on weekdays versus weekends. Mean weekday vehicle counts on the I-590 range from 98,000 to 115,000 throughout the year with 20–30% fewer vehicles on Saturdays and 40% less on Sundays, Fig. S4. The different day of week vehicle count pattern between the two sites reflects the size in the urban centers with roadways in the

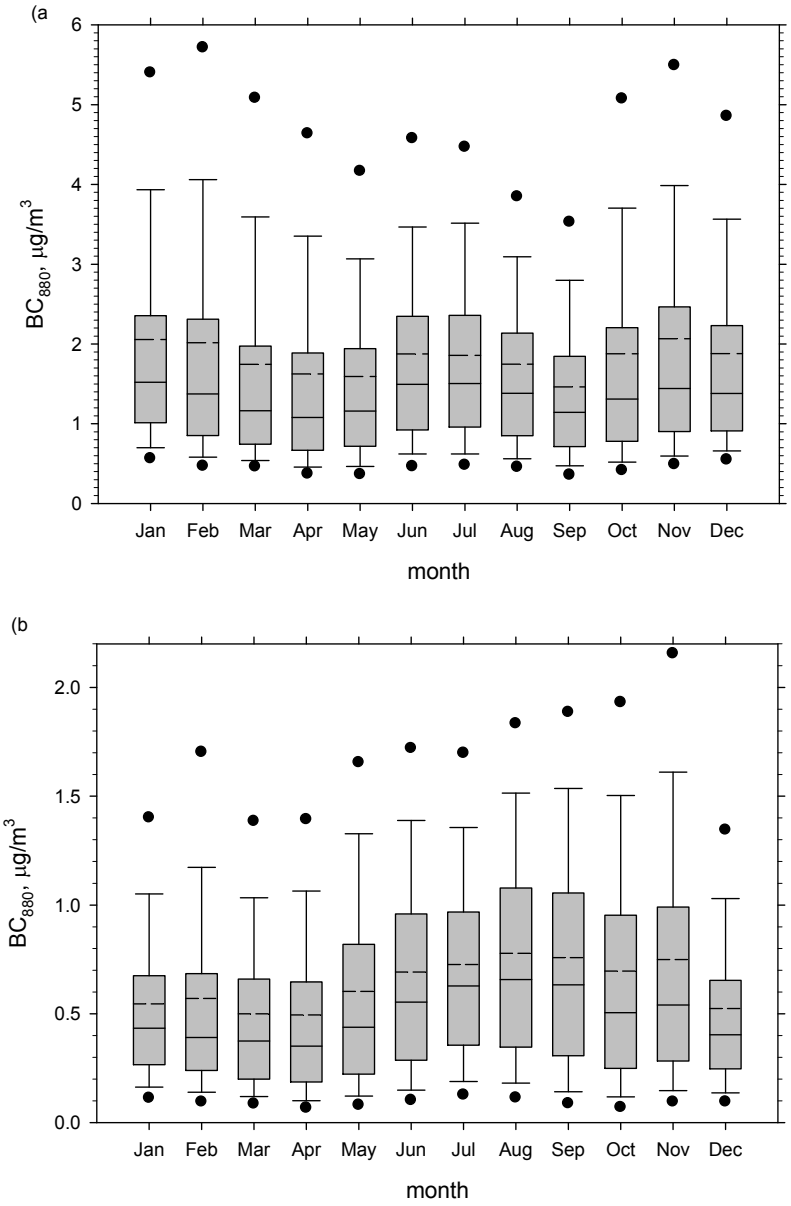

Fig. 4. Box and whisker plot of monthly BC_{880} concentrations in μg/m^3 at (a) the Bronx and (b) Rochester, NY. Symbol key as for Fig. 3.

larger NYC urban center experiencing a more uniform total daily number of vehicles throughout the week. Elevated BC was observed during weekdays at other urban sites (Baxla *et al.*, 2009; Saha and Despiau, 2009; Cheng *et al.*, 2012; Swamy *et al.*, 2012). Lough *et al.*, (2006) found elevated EC and motor vehicle molecular markers during weekdays at Los Angeles.

Diurnal Pattern

The weekday BC_{880} diurnal pattern at the Bronx reveals an increase in the morning concentration starting around 5 am with a peak between 7–9 am and a minimum in the early afternoon followed by a late evening gradual rise, Fig. 7. Although the range in concentrations varies across seasons a consistent overall weekday diurnal pattern is observed. Seasonal differences are attributed to differences in emissions, different sources coupled with variations in boundary layer height across seasons, Fig. S5. A similar diurnal pattern is observed for EC and NO_x but not SO_4 or OC which are dominated by secondary formation process, particularly in summer, as shown in Fig. S6. The diurnal profile on Saturdays shows a reduced morning maximum whereas on Sundays the morning peak is absent with highest concentrations at night, Fig. 8(a). To understand these BC_{880} patterns we need to look at both vehicle counts and boundary layer height. Fig. 8(b) shows mean hourly vehicle counts on the nearby Bruckner expressway. The weekday morning increase in BC_{880} coincides with a rapid rise in vehicle counts starting around 4–5 am. There is an 8-fold increase in hourly vehicle counts from 1000 vehicles per hour at 4 am to the peak of around 8,200–8,400 vehicles between 7–8 am. Vehicle counts subsequently decrease

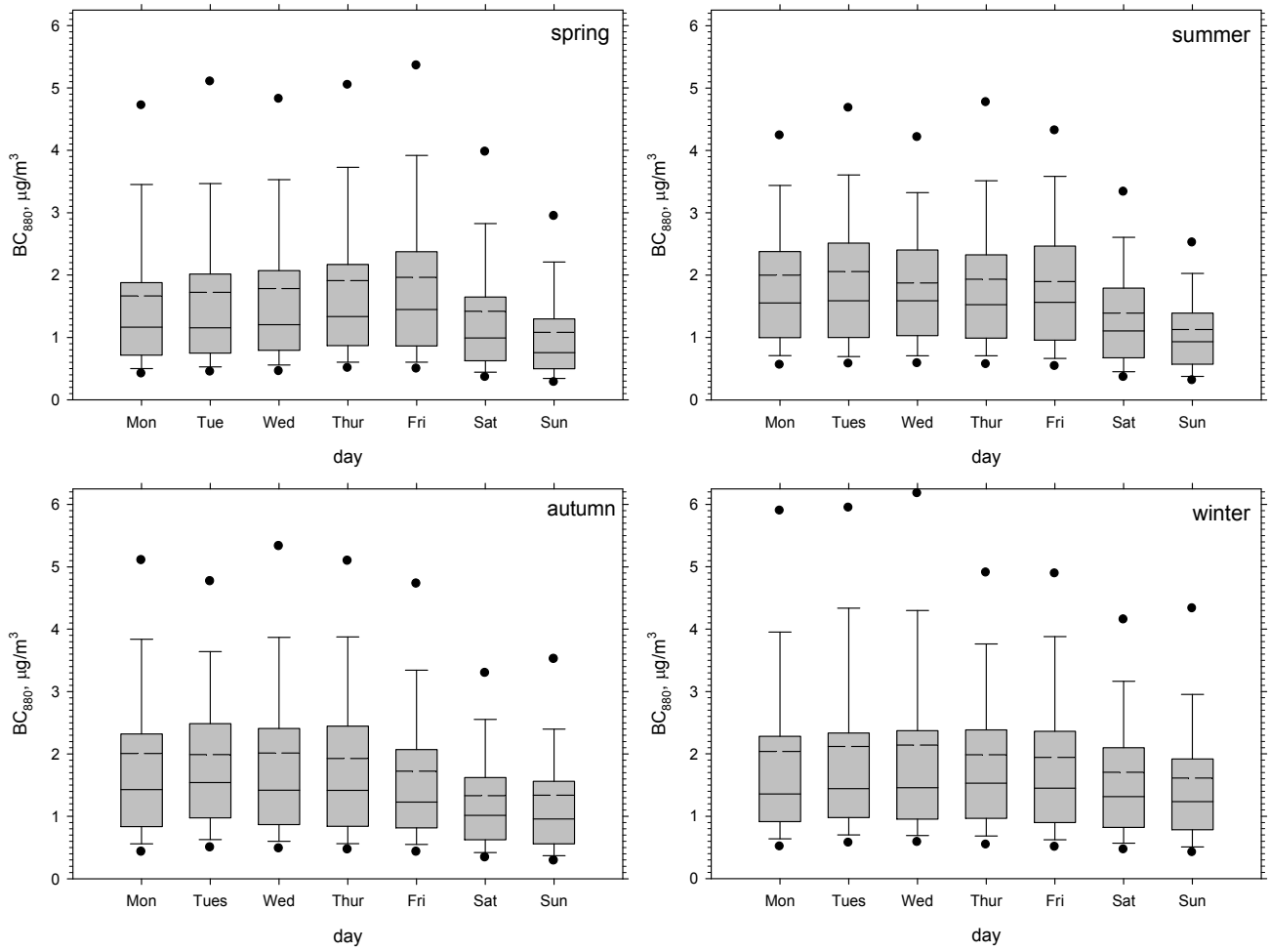

Fig. 5. Box and whisker plot showing the day of week BC_{880} concentration versus season at the Bronx. Symbol key as for Fig. 3.

before leveling off around 6,700 between 10 AM and noon (a 20% decrease compared to the peak) followed by a slow gradual afternoon rise with a broad secondary maximum between 2–4 PM. Although the total vehicle count may vary with season and also with the roadway size, there is a consistent diurnal traffic count profile throughout the year. The late morning and early afternoon decrease in BC_{880} (and NO_x shown in Fig. S6) amounts to approximately a factor of two variation with respect to the maximum. By comparison since vehicle counts only vary by approximately 20% on the nearby highway, the bulk of the morning pollutant decrease is attributed to an increase in boundary layer height (Fig. 8(c)). The variation in boundary layer height driven by solar heating is accompanied by increased wind speed and atmospheric turbulence leading to a dilution and dispersion of pollutants during the day. The boundary layer height remains elevated into the evening hours which is the reason for the absence of a secondary BC_{880} maximum during the afternoon and evening commute. A gradual rise in BC_{880} and NO_x is observed as the boundary layer collapses and pollution dispersion decreases in the evening hours despite the drop in vehicle counts. On Saturdays, there is a slower rise in vehicle counts compared to weekdays with no early morning peak but rather a broad maximum extending from around noon to 7 PM. Therefore, by the time traffic counts reaches its peak on Saturdays, the boundary layer has already expanded, and thus the influx of fresh pollutants is dispersed. On Sundays, there is a further lag in traffic growth which starts an hour or two later compared to weekdays and there is little or no morning BC_{880} peak.

The diurnal pattern at Rochester is similar although the late evening peak approaches the magnitude of the morning maximum particularly in summer and autumn, Fig. S7. Differences predominantly in the vehicle count profile and emission sources coupled with boundary layer dynamics are attributed to the differences in the late evening BC_{880} patterns between the two locations. Therefore, the timing of the morning traffic growth in relation to the boundary layer dynamics explains the different BC_{880} diurnal pattern on a weekday versus a weekend and the seasonal variation in BC_{880} diurnal profile. This also explains the weekday to weekend differences described in the previous section.

Similar diurnal profiles were observed at other urban locations (Park *et al.*, 2006; Baxla *et al.*, 2009; Saha and Despiau, 2009; Cheng *et al.*, 2012; Swamy *et al.*, 2012) although in some instances (Swamy *et al.*, 2012) the weekday to weekend differences may not be as large as observed in New York.

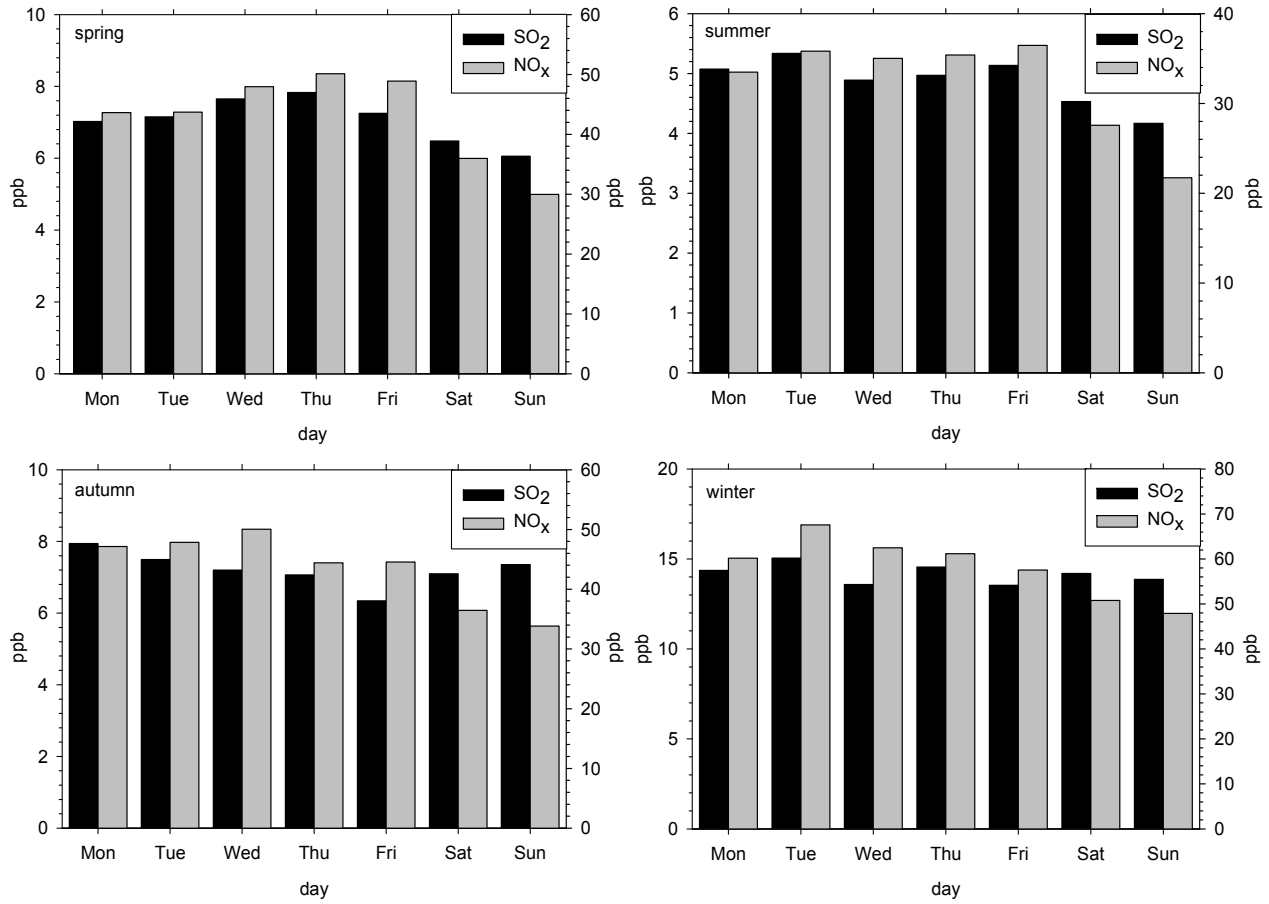

Fig. 6. Mean day of week concentration of NO_x (shaded box, right axis) and SO_2 (filled box, left axis) in ppb versus season at the Bronx.

Winter Pollution Episode

As previously mentioned, on average BC_{880} amounts to 14–20% of the $PM_{2.5}$ mass at the Bronx. However, during periods dominated by primary pollutants, BC_{880} can account for a much higher proportion of $PM_{2.5}$ mass. A pollution event occurred on February 22, 2007 during a winter inversion characterized by temperatures near 0^0C and wind speeds below 1 m/s, Fig. 9. Pollutant concentrations rose sharply during the early morning with $PM_{2.5}$ mass peaking close to 60 μg/m^3, BC_{880} near 20 μg/m^3 and total NO_x of 570 ppb between 6 and 7 AM. Prior to 2 AM, BC_{880} was around 15% of $PM_{2.5}$ mass but this increased to 30–38% between 4 and 8 AM. Many of the pollutants were correlated typical of an event dominated by primary pollutants. For example, BC was highly correlated with EC and NO_x, R^2 above 0.97, but also with $PM_{2.5}$ mass, R^2 of 0.94. A linear regression of OC and EC (excluding two points around the 7 AM peak when EC was higher than OC by 15–25%) showed an R^2 of 0.93 and a mean OC/EC ratio of 1.1 characteristic of primary OC/EC combustion ratios. After 7 AM, the temperature and wind speed increased and pollutants dispersed. Particle nitrate, however, which was relatively stable at around 2 μg/m^3 prior to 8 AM, rose sharply reaching a peak of 14 μg/m^3 around 11 AM, likely the result of photochemical oxidation of the large amount of NO_x. Pollutant concentrations were low in the early afternoon from 12–2 PM but concentrations increased again as the wind speed dropped showing a secondary but lower peak, $PM_{2.5}$ mass of 20 μg/m^3, around 6–8 PM.

Specific Source Markers

Previous Aethalometer® measurements showed that enhanced absorption at 370 nm relative to 880 nm (BC_{370} − BC_{880} = Delta C) tracked wood smoke markers, Levoglucosan and elemental potassium at the Rochester site (Wang *et al.*, 2011b) although Delta C is not a quantitative measure of mass concentration. This enhanced Delta C signal is evident from October to March at both sites (Fig. S8) but particularly during the late evening hours on weekends at Rochester (Fig. S9b) when residential wood burning is prominent and Delta C can reach several μg/m^3. An example of an event is shown in Fig. S10 on the weekend of Nov. 1–2, 2008 when Delta C peaked near 5.5 μg/m^3 around 9 PM on Saturday evening. BC_{880}, $PM_{2.5}$ mass and CO showed co-incidental peaks of around 4, 24 μg/m^3 and 1 ppm, respectively. This event is typical of winter weekend nocturnal pollution episodes when ambient temperatures drop below zero °C during the night and light winds from a southerly direction cause wood smoke emissions to advect towards the monitoring site leading to hourly Delta C of several μg/m^3 (Wang *et al.*, 2012). In contrast a weaker Delta C signal is observed at the Bronx site with mean late evening Delta C

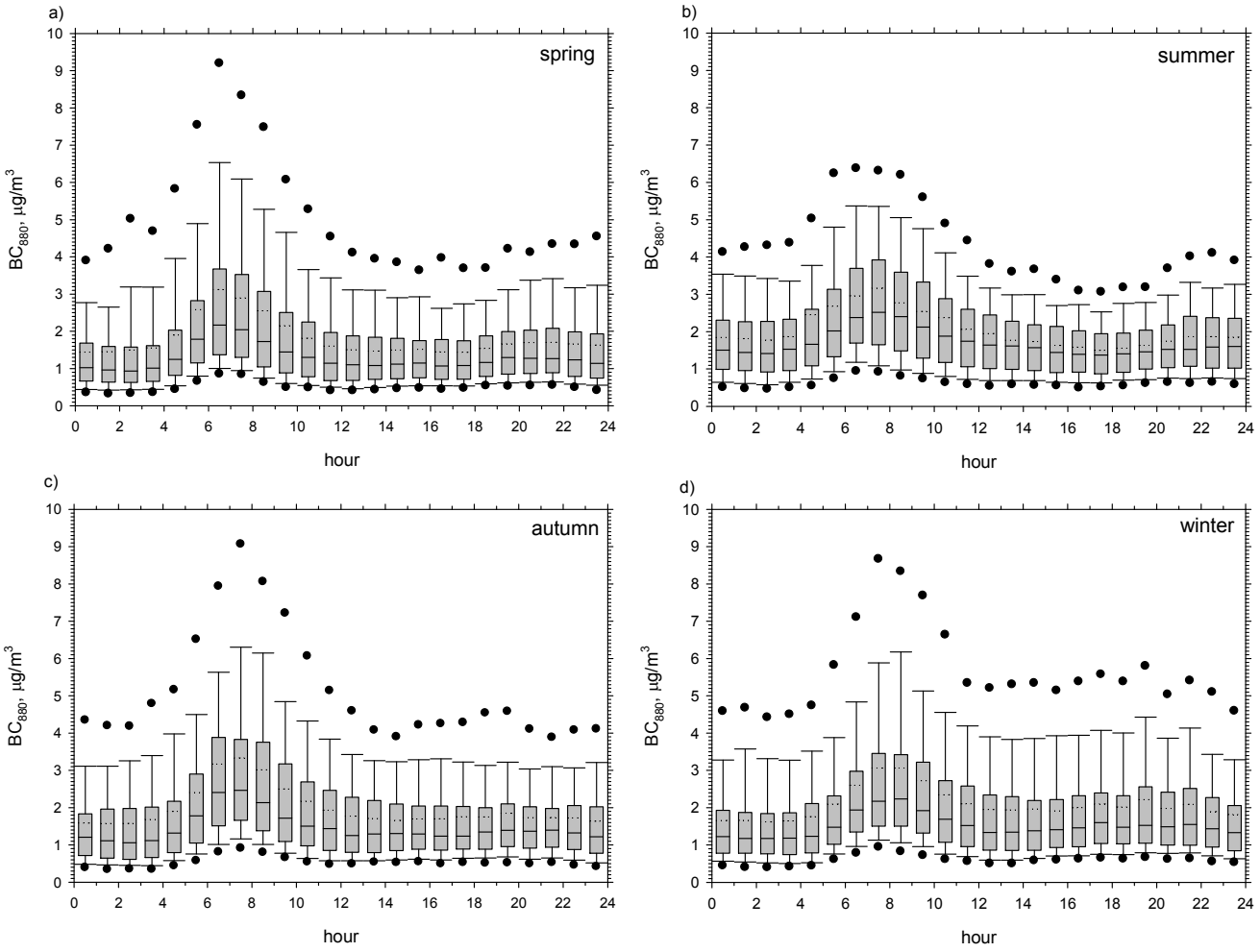

Fig. 7. Box and whisker plot showing the weekday diurnal BC_{880} concentration versus season at the Bronx. Symbol key as for Fig. 3.

values ~0.2 µg/m^3 in winter, Fig. S9(a). On the other hand, measurements of PM_{10} trace elements show elevated nickel (Ni) during the heating season at the Bronx site, Fig. 10(a). Mean winter Ni concentrations of 17.6 ng/m^3 are approximately a factor of 3 higher than in summer, 6.2 ng/m^3 consistent with earlier findings by Lippmann (2009). In addition a linear regression of Ni and Co (cobalt), Fig. 10(b), shows a mean Ni:Co ratio of 12.2 (for screened data with Co 2 ng/m^3 or below) close to the ratio of 14 observed in residual oil number 6, used for home heating in the Northeastern US (Graham, 2010). The large scatter in the Ni to Co relationship reflects different sources (for example different grade heating fuels or impact from other sources). Observations at rooftop level in the Bronx reveals frequent puffs of black smoke from building stacks, Fig. S11. These emissions which are attributed to the cycling on and off of oil boilers reveal hourly BC concentrations above 40 µg/m^3 (Rattigan *et al.*, 2010). At Rochester, Ni concentrations are a factor of 5–20 lower than at the Bronx with no winter/ summer concentration gradient. Natural gas and wood rather than fuel oil (number 4 and 6) are the predominant heating sources in the mainly single dwelling residences at Rochester. By contrast much of the surrounding residential area in the Bronx is high rise apartment blocks employing old style boilers burning residual oil for space and water heating as previously noted by Lippmann (2009).

Black Carbon vs. Elemental Carbon

As shown above BC_{880} was correlated with EC and NO_x with a diurnal pattern indicative of emissions from traffic sources. However, it is known that the relationship between BC_{880} and EC can vary depending on the particle composition (Jeong *et al.*, 2004; Kim *et al.*, 2006; Park *et al.*, 2006; Salako *et al.*, 2012). Jeong *et al.* (2004) and Kim *et al.* (2006) reported that the BC/EC relationship varied depending on the source and physical and chemical properties of the aerosol. Salako *et al.* (2012) analyzed the BC to EC relationship at various locations across Asia and the South Pacific. BC was measured by reflectrometry whereas EC was determined using the IMPROVE method (Chow *et al.*, 2007). Mean BC/EC ratios varied from a minimum of 0.47 for a rural site in Australia to a maximum of 3.56 for Bangkok, Thailand. Correlations were lowest for Malaysia, Bangkok and Australia and highest for Bangladesh and New Zealand. The authors attributed these results to differences in particle light absorptivity resulting from differences in

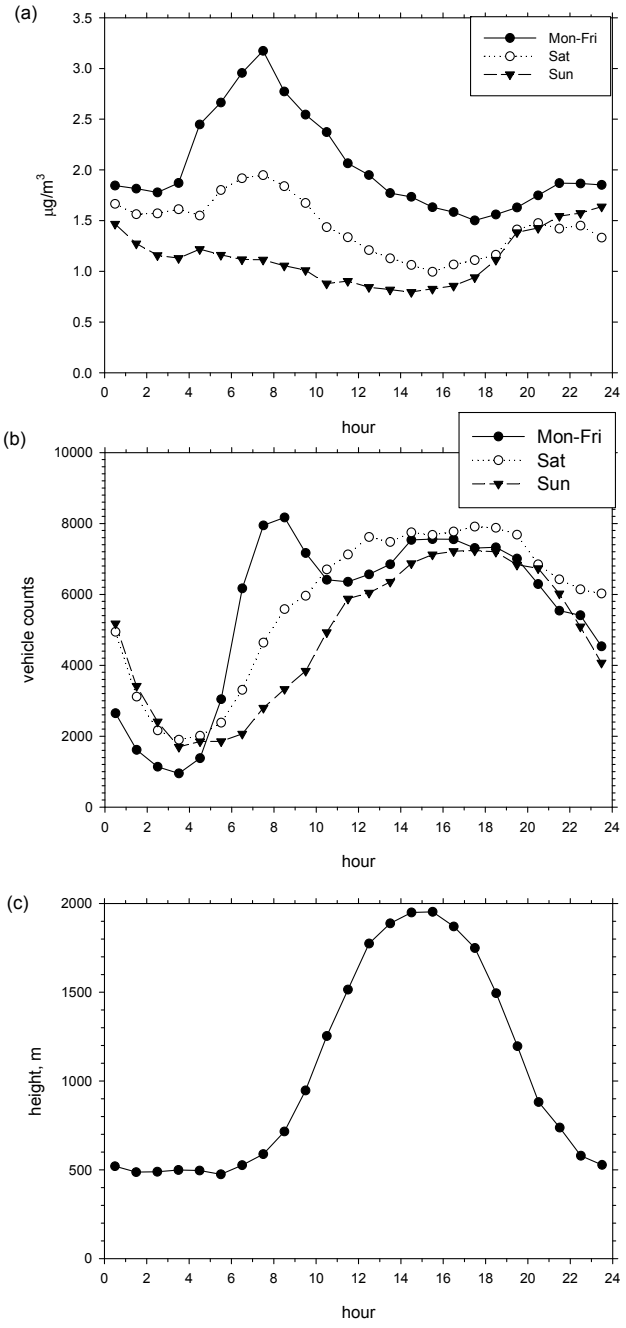

Fig. 8. Mean diurnal profile of (a) BC_{880}, (b) traffic counts and (c) boundary layer height during summer at the Bronx.

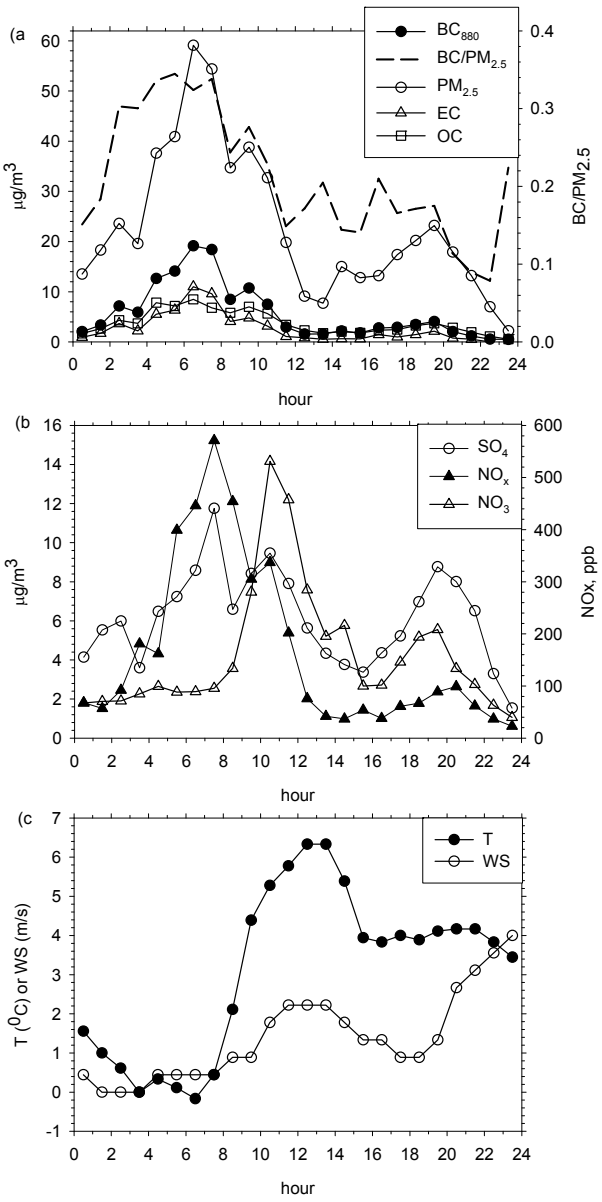

Fig. 9. Winter pollution episode showing of (a) BC_{880}, $PM_{2.5}$ mass, EC, OC and $PM_{2.5}/BC_{880}$ ratio, (b) SO_4, NO_3 and NO_x and (c) ambient temperature and wind speed during February 22, 2007 at the Bronx.

ambient source contributions (biomass burning versus vehicular emissions) and degree of atmospheric processing. Here two methods were used in the comparison of BC_{880} and EC; (1) BC/EC ratios and (2) a robust linear regression of BC_{880} and EC. The long term trends show that the annual ratio of BC_{880} to EC and BC_{880} to TC measured by the CSN TOT method (Peterson and Richards, 2002) at the Bronx varied from 1.4 to 1.8 and 0.4 to 0.5, respectively. The corresponding ratios at Rochester were 1.4 to 1.6 and 0.2 to 0.3, respectively. Monthly ratios of BC_{880} to EC measured by the CSN TOT and IMPROVE TOR (Chow *et al.*, 2007) methods are shown in Figs. 11(a) and 11(b), respectively. At both sites the ratio of BC_{880} to EC analyzed using the TOT method, Fig. 11(a), is elevated in summer (June to August) compared to winter. The mean ratio is 1.3 with a standard deviation of 0.3 from October to March increasing to a ratio of 1.8 with a standard deviation of 0.2 from June to August. In contrast the ratio of BC_{880} to IMPROVE EC, Fig. 11(b), shows little seasonal gradient at the Bronx site with a mean annual ratio of 1.3 close to the ratio of 1.4 for the EC CSN TOT method during winter. The ratio of BC to IMPROVE EC at Rochester is similar except for the month of June when it is below 1. Note that in the case of Rochester, the IMPROVE carbon protocol was introduced in April 2009 and therefore does not extend over the same sampling period as the CSN TOT data.

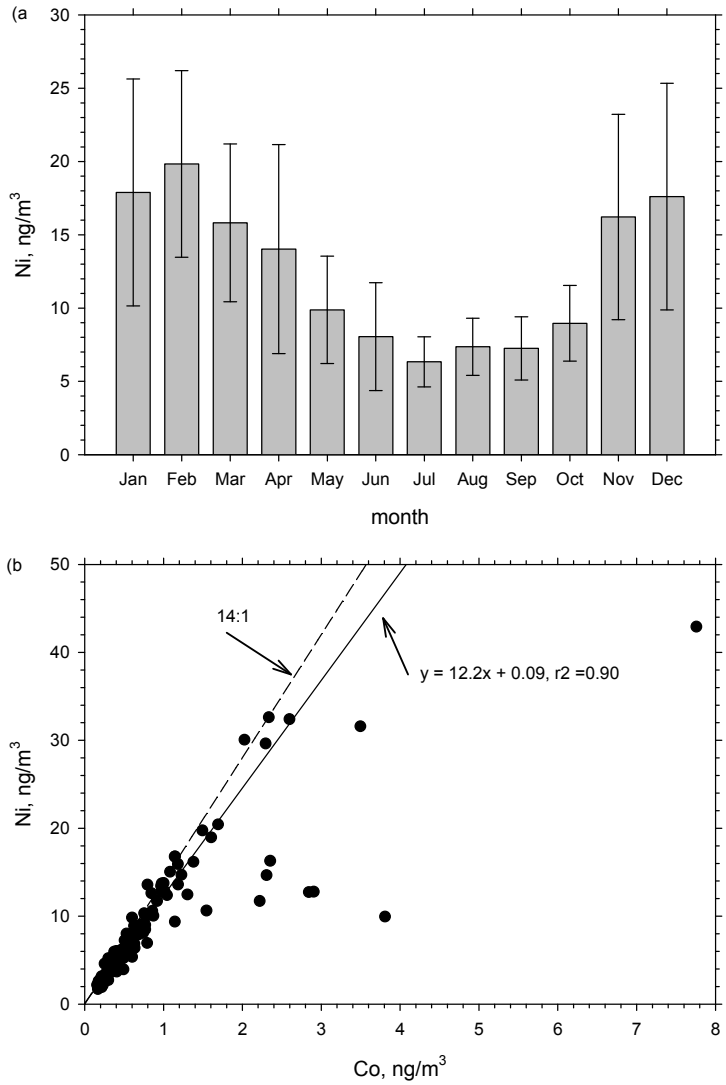

Fig. 10. Concentrations of elemental Ni with 95% confidence limits versus season in 24h PM_{10} samples at the Bronx (a) and the relationship between Ni and Co (b). The solid line in (b) is a regression fit of data at or below 2 ng/m^3 Co and the dashed line represents a ratio of 14:1 observed in residual oil number 6 (Graham, 2010).

Results of the robust linear regressions of BC_{880} with the various EC methods are shown in Table 3 and 4. Seasonal regression coefficients and the combined results are provided. At the Bronx the regression slopes reflect the pattern observed in the BC_{880}/EC ratios. Thus slopes are above unity with generally higher values in summer for the comparison with the EC TOT methods (MetOne, R&P 2300). For example the slope in summer is 64% higher compared to winter for the MetOne comparison versus 30% higher for the R&P 2300. However, except for the MetOne, the seasonal differences overlap within the uncertainties. Regression slopes for the comparison of BC_{880} with EC analyzed by the IMPROVE TOR (URG-3000N) vary between 1.31 to 1.44 showing seasonal differences of 10%. In all cases correlation coefficients, R, are above 0.8 and intercepts are zero or close to zero within the uncertainties. Regression slopes for comparison of BC_{880} and EC analyzed using TOT (MetOne, R&P 2300) at Rochester are similar in magnitude to the Bronx. However, slopes show less of a summer/winter contrast, 22–24% at Rochester compared to 30–64% the Bronx. The regression slopes for BC_{880} and TOR EC at Rochester are unity within the uncertainties and approximately 30–40% lower than observed at the Bronx. The variation in the BC_{880}/EC relationship with location and season is consistent with a change in optical properties of the ambient particle which impact optical measurement of BC as indicated in previous findings (Petzold *et al.*, 1997; Jeong *et al.*, 2004; Park *et al.*, 2006; Salako *et al.*, 2012). Thus assuming a fixed absorption coefficient may be incorrect (Petzold *et al.*, 1997). The resultshere also show that the BC_{880}/EC relationship depends on the EC measurement method used consistent with their method dependent definitions.

CONCLUSIONS

Measurements of BC_{880} over multiple years were used to characterize temporal patterns on an annual, seasonal, day

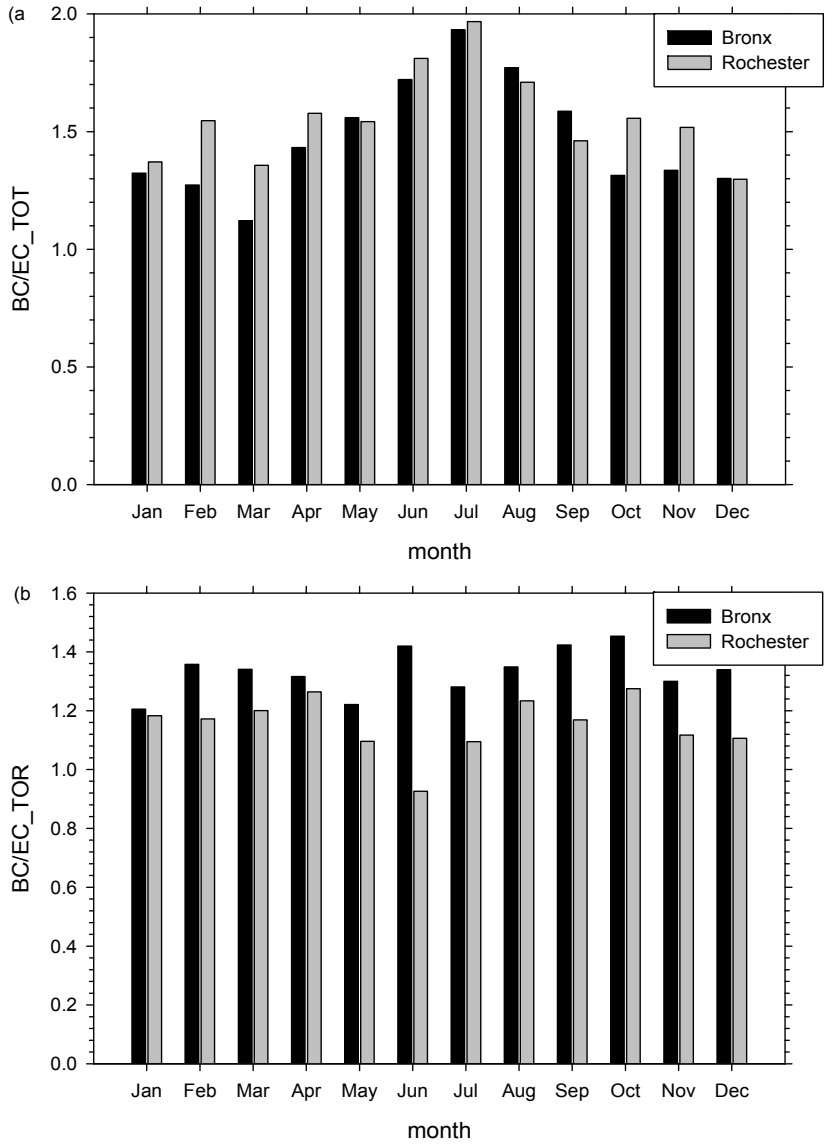

Fig. 11. Ratio of BC_{880}/EC at the Bronx (filled box) and Rochester (shaded) versus season for TOT (a) and TOR (b) EC measurement methods.

of week and diurnal basis at two urban locations in New York. Annual mean BC_{880} concentrations in New York City ranged from 1.4 to 2.0 μg/m^3 and were a factor of 2–3 lower at Rochester. Similar day of week and diurnal patterns are attributed to traffic emissions from nearby roadways at both sites. Higher weekday (Monday–Friday) BC_{880} concentrations compared to weekends (Saturday and Sunday) results from increased vehicle emissions prior to the expansion of the boundary layer during the morning workday commute. Weekend vehicle emissions lag those on weekdays and evolve as the boundary expands resulting in their dilution and dispersion. The effect is most evident on Sundays as indicated in the lack of a morning BC_{880} peak. Dual wavelength BC measurements showed an enhanced DeltaC = $BC_{370} - BC_{880}$ signal from October to March predominantly during late evening weekend hours at Rochester. In contrast a weaker DeltaC signal was observed at the Bronx location. However, Ni and Co were elevated in PM_{10} samples during the heating season at the Bronx site since residual oil rather than wood or natural gas is used as a heating fuel source. In addition the ratio of Ni to Co was close to the ratio found in residual oil number 6. Comparison of BC_{880} with EC showed an enhancement in the BC_{880}/EC ratio during summer compared to winter for thermal optical transmission methods, particularly at the Bronx where summer BC_{880}/EC ratios were 30–60% higher compared to winter. By contrast the BC_{880}/EC ratio showed little seasonal variation for the EC IMPROVE thermal optical reflectance method.

ACKNOWLEDGMENTS

The authors wish to thank Richardson Colas, and Michael Abbott for help with instrument operation at the South Bronx and Tom Everts for assistance at the Rochester site.

Table 3. Robust linear regression coefficients and 1 σ uncertainties for comparison of BC_{880} and EC from various methods at the Bronx site.

(a) Comparison of BC_{880} and MetOne TOT EC at the Bronx site.

season	slope	intercept	R	N
Spring	(1.46 ± 0.14)	–(0.23 ± 0.18)	0.90	89
Summer	(1.93 ± 0.31)	–(0.39 ± 0.34)	0.82	71
Autumn	(1.38 ± 0.16)	–(0.09 ± 0.20)	0.98	61
Winter	(1.18 ± 0.13)	–(0.15 ± 0.23)	0.96	67
all	(1.37 ± 0.08)	–(0.11 ± 0.10)	0.91	288

(b) Comparison of BC_{880} and R&P2300 TOT EC at the Bronx site.

season	slope	intercept	R	N
Spring	(1.72 ± 0.21)	–(0.45 ± 0.27)	0.94	60
Summer	(2.03 ± 0.30)	–(0.16 ± 0.33)	0.88	66
Autumn	(1.67 ± 0.13)	–(0.30 ± 0.25)	0.81	73
Winter	(1.57 ± 0.28)	–(0.29 ± 0.39)	0.89	50
all	(1.77 ± 0.12)	–(0.31 ± 0.10)	0.86	249

(c) Comparison of BC_{880} and IMPROVE TOR EC at the Bronx site.

season	slope	intercept	R	N
Spring	(1.40 ± 0.10)	–(0.25 ± 0.13)	0.92	177
Summer	(1.37 ± 0.12)	–(0.15 ± 0.17)	0.88	161
Autumn	(1.44 ± 0.11)	–(0.15 ± 0.13)	0.89	172
Winter	(1.31 ± 0.10)	–(0.26 ± 0.16)	0.86	169
all	(1.35 ± 0.05)	–(0.17 ± 0.07)	0.88	679

Table 4. Robust linear regression coefficients and 1 σ uncertainties for comparison of BC_{880} and EC from various methods at Rochestrer.

(a) Comparison of BC_{880} and MetOne TOT EC at Rochester.

season	slope	intercept	R	N
Spring	1.78 ± 1.06	–0.16 ± 0.45	0.89	25
Summer	1.69 ± 1.14	–0.08 ± 0.63	0.83	21
Autumn	1.70 ± 0.64	–0.20 ± 0.39	0.79	40
Winter	1.36 ± 0.65	–0.07 ± 0.32	0.64	52
all	1.61 ± 0.38	–0.14 ± 0.20	0.78	138

(b) Comparison of BC_{880} and R&P2300 TOT EC at Rochester.

season	slope	intercept	R	N
Spring	1.96 ± 0.57	–0.16 ± 0.24	0.90	80
Summer	2.10 ± 0.65	–0.11 ± 0.29	0.74	98
Autumn	1.91 ± 0.41	–0.17 ± 0.23	0.89	96
Winter	1.71 ± 0.49	–0.10 ± 0.22	0.83	78
all	1.93 ± 0.25	–0.14 ± 0.12	0.84	352

(c) Comparison of BC_{880} and IMPROVE TOR EC at Rochester.

season	slope	intercept	R	N
Spring	1.03 ± 0.25	–0.03 ± 0.11	0.90	100
Summer	1.14 ± 0.32	–0.03 ± 0.18	0.87	75
Autumn	1.15 ± 0.23	–0.00 ± 0.13	0.94	83
Winter	1.27 ± 0.29	–0.03 ± 0.13	0.99	77
all	1.14 ± 0.13	–0.01 ± 0.06	0.93	335

DISCLAIMER

The opinions expressed in this paper do not necessarily reflect the views of New York State Department of Environmental Conservation.

SUPPLEMENTARY MATERIALS

Supplementary data associated with this article can be found in the online version at http://www.aaqr.org.

REFERENCES

Albrecht, B.A. (1989). Aerosols, Cloud Microphysics and Fractional Cloudiness. *Science* 245: 1227–1230.

Arnott, W.P., Hamasha, K., Moosmuller, H., Sheridan, P.J. and Ogren, J.A. (2005). Towards Aerosol Light-Absorption Measurements with a 7-Wavelength Aethalometer: Evaluation with a Photoacoustic Instrument and 3-Wavelength Nephelometer. *Aerosol Sci. Technol.* 39: 17–29.

Baxla, S.P., Roy, A.A., Gupta, T., Tripathi, S.N. and Bandyopadhyaya, R. (2009). Analysis of Diurnal and Seasonal Variation of Submicron Outdoor Aerosol Mass and Size Distribution in a Northern Indian City and Its Correlation to Black Carbon. *Aerosol Air Qual. Res.* 9: 458–469.

Begum, B.A., Hossain, A., Nahar, N., Markwitz, A. and Hopke, P.K. (2012). Organic and Black Carbon in $PM_{2.5}$ at an Urban Site at Dhaka, Bangladesh. *Aerosol Air Qual. Res.* 12: 1062–1072.

Birch, M.E. and Cary, R.A. (1996). Elemental Carbon-based Method for Monitoring Occupational Exposures to Particulate Diesel Exhaust. *Aerosol Sci. Technol*. 25: 221–241.

Bond, T.C., Anderson, T.L. and Campbell, D. (1999). Calibration and Intercomparison of Filter-based Measurements of Visible Light Absorption by Aerosols. *Aerosol Sci. Technol.* 30: 582–600.

Bond, T.C., Bhardwaj, E., Dong, R., Jogani, R., Jung, S., Roden, C., Streets, D.G. and Trautmann, N.M. (2007). Historical Emissions of Black and Organic Carbon Aerosol from Energy-related Combustion, 1850–2000. *Global Biogeochem. Cycles* 21: GB2018, 1–16.

Cheng, Y., Ho, K.F., Wu, W.J., Ho, S.S.H., Lee, S.C., Huang, Y., Zhang, Y.W., Yao, P.S., Gao, Y. and Chan, C.S. (2012). Real-Time Characterization of Particle-Bound Polycyclic Aromatic Hydrocarbons at a Heavily Trafficked Roadside Site. *Aerosol Air Qual. Res.* 12: 1181–1188.

Chow, J.C., Watson, J.G., Chen, L.W.A., Chang, M.C.O., Robinson, N.F., Trimble, D. and Kohl, S. (2007). The IMPROVE_A Temperature Protocol for Thermal Optical Carbon Analysis: Maintaining Consistency with a Long-Term Database. *J. Air Waste Manage. Assoc.* 57: 1014–1023.

Cornell, A.G., Chillrud, S.N., Mellins, R.B., Acosta, L.M., Miller, R.L., Quinn, J.W., Yan, B., Divjan, A., Olmedo, O.E., Lopez-Pintado, S., Kinney, P.L., Perera, F.P., Jacobson, J.S., Goldstein, I.F., Rundle, A.G. and Perzanowski, M.S. (2012). Domestic Airborne Black Carbon and Exhaled Nitric Oxide in Children in NYC. *J. Exposure Sci. Environ. Epidemiol.* 22: 258–266.

Doraiswamy, P., Hogrefe, C., Hao, W., Civerolo, K., Ku, J.Y. and Gopal Sistla, G. (2010). A Retrospective Comparison of Model-Based Forecasted $PM_{2.5}$ Concentrations with Measurements. *J. Air Waste Manage. Assoc.* 60: 1293–1308.

Graham, J. (2010). Select Trace Elemental Composition of Fuel Oil used in the Northeastern United States, EM Magazine, Air & Waste Management Association, p. 16–22.

Hansen, A.D.A., Rosen, H. and Novakov, T. (1984). The Aethalometer -An Instrument for the Real-time Measurement of Optical Absorption by Aerosol Particles. *Sci. Total Environ*. 36: 191–196.

Hildemann, L.M., Markowski, G.R., Jones, M.C., Cass, G.R. (1991). Submicrometer Aerosol Mass Distribution of Emissions from Boilers, Fireplaces, Automobiles, Diesel Trucks, and Meat Cooking Operations. *Aerosol Sci. Technol*. 14: 138–152.

Intergovernmental Panel on Climate Change (2007). Climate Change 2007: The Physical Science Basis. Contribution of Working Group I to the Fourth Assessment, *Report of the Intergovernmental Panel on Climate Change*, Solomon, S. *et al.*, (Eds.), Cambridge Univ. Press, Cambridge, U.K.

Jacobson, M.Z. (2002). Control of Fossil-Fuel Particulate Black Carbon and Organic Matter, Possibly the Most Effective Method of Slowing GlobalWarming. *J. Geophys. Res.* 107: 4410, doi: 10.1029/2001JD001376.

Janjic, Z.I. (2001). Nonsingular Implementation of the Mellor-Yamada Level 2.5 Scheme in the NCEP Meso Mode, NCEP Office Note No. 437, p. 1–61.

Jeong, C.H., Hopke, P.K., Kim, E. and Lee, D.W. (2004). The Comparison between Thermal-optical Transmittance Elemental Carbon and Aethalometer Black Carbon Measured at Multiple Monitoring Sites. *Atmos. Environ.* 38: 5193–5204.

Kim, J.J., Smorodinsky, S., Lipsett, M., Singer, B.C., Hodgson, A.T. and Ostro B. (2004). Traffic-related Air Pollution near Busy Roads The East Bay Children's Respiratory Health Study. *Am. J. Respir. Crit. Care Med.* 170: 520–526.

Kim, Y.J., Kim, M.J., Lee, K.H. and Park, S.S. (2006). Investigation of Carbon Pollution Episodes Using Semi-continuous Instrument in Incheon, Korea. *Atmos. Environ.* 40: 4064–4075.

Kirchstetter, T., Novakov, T. and Hobbs, P. (2004). Evidence that Spectral Light Absorption by Aerosols Emitted by Biomass Burning and Motor Vehicles is Different due to Organic Carbon. *J. Geophys. Res*. 109: D21208.

Liousse, C, Cachier, H. and Jennings, S.G. (1993). Optical and Thermal Measurements of Black Carbon Aerosol Content in Different Environments: Variations of the Specific Attenuation Cross-section, Sigma(s). *Atmos. Environ.* 27A: 1203–1211.

Lippmann, M. (2009). Semi-continuous Speciation Analysis for Ambient Air Particulate Matter: An Urgent Need for Health Effects Studies. *J. Exposure Sci. Environ. Epidemiol.* 19: 235–247.

Lough, G.C., Schauer, J.J. and Lawson, D.R. (2006). Day of Week Trends in Carbonaceous Aerosol Composition in the Urban Atmosphere. *Atmos. Environ.* 40: 4137–4149.

Malm, W.C., Sisler, J.F., Huffman, D., Eldred, R.A. and Cahill, T.A. (1994). Spatial and Seasonal Trends in Particle Concentration and Optical Extinction in the US. *J. Geophys. Res*. 99: 1347–1370.

Park, K., Chow, J.C., Watson, J.G., Trimble, D.L.,

Doraiswamy, P., Park, K., Arnott, W.P., Stroud, K.R., Bowers, K., Bode, R., Petzold, A. and Hansen, A.D.A. (2006). Comparison of Continuous and Filter-Based Carbon Measurements at the Fresno Supersite. *J. Air Waste Manage. Assoc.* 56: 474–491.

Park, S.S., Hansen, A.D.A., Sung, Y. and Cho, S.Y. (2010). Measurement of Real Time Black Carbon for Investigating Spot Loading Effects of Aethalometer Data. *Atmos. Environ.* 44: 1449–1455.

Peterson, M.R. and Richards, M. H. (2002). In Winegar, E.D. and Tropp, R.J. (Eds.), Thermal-Optical Transmittance Analysis for Organic, Elemental, Carbonate, Total Carbon, and OCX2 in $PM_{2.5}$ by the EPA/NIOSH Method, Proceedings, Symposium on Air Quality Measurement Methods and Technology, 83-1-83-19.

Petzold, A., Kopp, C. and Niessner, R. (1997). The Dependence of the Specific Attenuation Cross-Section On Black Carbon Mass Fraction and Particle Size. *Atmos. Environ*. 31: 661–672.

Petzold, A., Kramer, H. and Schönlinner, M. (2002). Continuous Measurement of Atmospheric Black Carbon Using a Multi-Angle Absorption Photometer. *Environ. Sci. Pollut. Res.* 4: 78–82.

Ramanathan, V. and Carmichael, G. (2008). Global and Regional Climate Changes due to Black Carbon. *Nat. Geosci.* 1: 221–227.

Rattigan, O.V., Felton, H.D., Bae, M.S., Schwab, J.J. and Demerjian, K.L. (2010). Multi-year Hourly $PM_{2.5}$ Carbon Measurements in New York: Diurnal, Day of Week and Seasonal Patterns. *Atmos. Environ.* 2043–2053.

Rattigan, O.V., Felton, H.D., Bae, M.S., Schwab, J.J. and Demerjian, K.L. (2011). Comparison of Long-term $PM_{2.5}$ Carbon Measurements at an Urban and Rural Location in New York, *Atmos. Environ.* 45: 3228–3236.

Saha, A. and Despiau, S. (2009). Seasonal and Diurnal Variations of Black Carbon Aerosols over a Mediterranean Coastal Zone. *Atmos. Res*. 92: 27–41.

Salako, G.O., Hopke, P.K., Cohen, D.D., Begum, B.A., Biswas, S.K., Pandit, G.G., Chung, Y.S., Rahman, S.A., Hamzah, M.S., Davy, P., Markwitz, A., Shagjjamba, D., Lodoysamba, S., Wimolwattanapun, W. and Bunprapob, S. (2012). Exploring the Variation between EC and BC in a Variety of Locations. *Aerosol Air Qual. Res.* 12: 1–7.

Schauer, J.J. (2003). Evaluation of Elemental Carbon as a Marker for Diesel Particulate Matter. *J. Exposure Sci. Environ. Epidemiol.* 13: 433–453.

Seinfeld, J.H. and Pandis, S.N. (1998). *Atmospheric Chemistry and Physics: From Air Pollution to Climate Change*, Wiley, New York, p. 700–763.

Swamy, Y.V., Venkanna, R., Nikhil, G.N., Chitanya, D.N.S.K., Sinha, P.R., Ramakriskna, M. and Rao, A.G. (2012). Impact of Nitrogen Oxides, Volatile Organic Compounds and Black Carbon on Atmospheric Ozone Levels at a Semi-Arid Urban site in Hyderabad. *Aerosol Air Qual. Res.* 12: 662–671.

Turner, J.R., Hansen, A.D.A. and Allen, G.A. (2007). Methodologies to Compensate for Optical Saturation and Scattering in Aethalometer Black Carbon Measurements, In *Symposium on Air Quality Measurement Methods and Technology*, San Francisco, CA. AWMA, Pittsburgh PA, Paper No. 37.

Virkkula, A., Makela, T., Hillamo, R., Tuomi, T.Y., Hirsikko, A., Hameri, K. and Koponen, I.K. (2007). A Simple Procedure for Correcting Loading Effects of Aethalometer Data. *J. Air Waste Manage. Assoc.* 57: 1214–1222.

Wallen, A., Liden, G. and Hansson, H.C. (2010). Measured Elemental Carbon by Thermo-Optical Transmittance Analysis in Water-Soluble Extracts from Diesel Exhaust, Woodsmoke and Ambient Particulate Samples. *J. Occup. Environ. Hyg.* 7: 35–45.

Wang Y., Hopke P.K., Chalupa, D.C. and Utell, M.J. (2010). Long-term Study of Urban Ultrafine Particles and other Pollutants. *Atmos. Environ*. 45: 7672–80.

Wang, Y., Hopke, P.K., Chalupa, D.C. and Utell, M.J. (2011a). Effect of the Shutdown of a Coal-fired Power Plant on Urban Ultrafine Particles and other Pollutants. *Aerosol Sci. Technol*. 45: 1245–49.

Wang, Y., Hopke, P.K., Rattigan, O.V., Xia, X., Chalupa, D.C. and Utell, M.J. (2011b). Characterization of Residential Wood Combustion Particles Using the Two-Wavelength Aethalometer. *Environ. Sci. Technol*. 45: 7387–7393.

Wang, Y., Hopke, P.K., Rattigan, O.V., Chalupa, D.C. and Utell, M.J. (2012). Multiple-year Black Carbon Measurements and Source Apportionment Using Delta-C in Rochester, New York. *J. Air Waste Manage. Assoc.* 62: 880–887.

Weingartner, E., Saatho, H., Schnaiterb, M., Streita, N., Bitnarc, B. and Baltensperger, U. (2003). Absorption of Light by Soot Particles: Determination of the Absorption Coefficient by Means of Aethalometers. *J. Aerosol Sci*. 34: 1445–1463.

Received for review, February 25, 2013
Accepted, May 22, 2013